Materials Advances

ROYAL SOCIETY OF CHEMISTRY

COMMUNICATION

View Article Online
View Journal | View Issue

Cite this: *Mater. Adv.*, 2021, 2, 6267

Received 6th August 2021,
Accepted 26th August 2021

DOI: 10.1039/d1ma00696g

rsc.li/materials-advances

Improving the *ZT* of SnTe using electronic structure engineering: unusual behavior of Bi dopant in the presence of Pb as a co-dopant

U. Sandhya Shenoy *[a] and D. Krishna Bhat *[b]

Electronic structure engineering of SnTe by doping various elements to improve its figure of merit has been the most promising approach recently sought after. Pb doped in SnTe is well known to decrease the thermal conductivity but fails to beneficially tune its electronic properties. Herein, we co-dope Bi in SnTe doped with Pb, to improve the power factor of the material. Bi in the presence of Pb exhibits unusual features not shown in the case of Bi doped SnTe. The synergistic action leads to an increase in the band gap and valence band convergence. Bi also introduces resonance states just below the conduction band edge and causes conduction band convergence. An enhanced power factor due to modification of the electronic structure combined with reduced thermal conductivity translates into an enhanced figure of merit of up to ~1.58 at 800 K as predicted using Boltzmann transport calculations, making it a potential thermoelectric material worthy of further study.

1. Introduction

Thermoelectric technology with the ability to scavenge waste heat and convert it into electrical energy is the most promising solid-state technology to reduce the consumption of fossil fuels and minimize the loss of energy during their consumption. SnTe, a rock salt analogue of PbTe has been receiving increasing attention due to its tunable crystal and electronic structure.[1–4] Pristine SnTe is considered a poor thermoelectric due to a large number of inherent vacancies, a low band gap and a high energy offset between its conduction and valence sub-bands, which results in a poor power factor. Also, SnTe possess a high thermal conductivity further reducing the figure of merit, *ZT* value. Various approaches have been implemented to reduce the thermal conductivity of SnTe like doping, introduction of interstitials, and nano structuring.[5–15] Among these, doping of Pb has led to substantial improvements of *ZT*.[12,13] A dual step approach has been implemented in the past to improve the power factor.[11] Mg and Cd are known to increase the band gap of SnTe and cause valence band convergence and In is known to introduce resonance levels.[2,16,17] Co-doping of these two classes of dopants *i.e.* Mg–In and Cd–In was reported to improve the power factor of Pb doped SnTe.[18,19] However the resulting *ZT* was found to be around 1 and 0.82. After the discovery of Zn as a versatile resonant dopant in SnTe, Zn was co-doped with Pb to simultaneously act as a resonant dopant as well as increase the band gap and cause hyperconvergence in the valence bands of Pb doped SnTe.[4,11] This led to the development of a promising p-type thermoelectric material with a *ZT* of 1.66 at 840 K.[11] Thermoelectric technology requires both p and n type materials with comparable performances for practical applications. Bi in SnTe was previously known to tune only the carrier concentration.[20] However recent studies have revealed Bi to be a successful n-type resonant dopant in SnTe.[21,22] Hence, we thought studying the effect of Bi doping in the presence of Pb in SnTe was worthwhile. The combined electronic structure and transport property studies using first principles calculations reveal the unusual synergistic nature of Bi and Pb in improving the thermoelectric properties of SnTe making it a suitable material for further experimental study.

2. Computational details

We used the Quantum ESPRESSO package for simulation of the electronic structures of SnTe; Pb doped and Pb–Bi co-doped SnTe configurations.[23] To capture the effect of spin orbit coupling relativistic pseudopotentials are necessary. Our DFT calculations involved fully relativistic ultrasoft pseudopotentials with Generalized Gradient Approximation (GGA) of the Perdew, Burke, and Erzenhoff (PBE) functional types.[24] The pseudopotentials included Sn ($4d^{10}5s^25p^2$), Te ($4d^{10}5s^25p^4$), Pb ($5d^{10}6s^26p^2$) and Bi ($5d^{10}6s^26p^3$) as the valence electrons. The

[a] *Department of Chemistry, College of Engineering and Technology, Srinivas University, Mukka, Mangalore – 574146, India. E-mail: sandhyashenoy347@gmail.com*
[b] *Department of Chemistry, National Institute of Technology Karnataka, Surathkal, Mangalore – 575025, India. E-mail: denthajekb@gmail.com*

supercells of $(\sqrt{2} \times \sqrt{2} \times 2)a_o$ dimensions containing 32 atoms were fully relaxed for the determination of total energies. The wavefunctions represented by the plane wave basis were truncated with cut off values of 50 Ry for energy and 400 Ry for charge density, respectively. A k mesh of $14 \times 14 \times 10$ points was used to sample the Brillouin zone integrations and the band structures were determined along the high symmetry lines (M–Γ–Z–R–A) in the Brillouin zone.

3. Results and discussion

The electronic structure of SnTe reveals a direct band gap of 0.081 eV at the Γ point due to the typical underestimation in DFT based calculations (Fig. 1a).[4,22] It is well known that PbTe and SnTe have inverted bands and the addition of Pb into SnTe gradually decreases the band gap to zero when Sn = 0.4 and Pb = 0.6.[25–27] When we simulate the electronic structure for a composition of $Sn_{0.7}Pb_{0.3}Te$, we observe that the system appears metallic as DFT fails to capture the extremely low band gap (Fig. 1b).[11] Although addition of Pb is known to decrease the lattice thermal conductivity favorably, the decrease in the band gap leads to onset of bipolar diffusion and hence has a negative impact on the power factor.[26,27] We know that Bi is an n-type resonant dopant in SnTe known to introduce resonance levels just beneath the conduction band and improve the room temperature Seebeck co-efficient.[21,22,28] Hence, we co-doped Bi to beneficially tune the electronic structure. In the electronic structure of Pb–Bi co-doped SnTe, we observe an increase of 0.147 eV in the band gap at the Γ point, effectively solving the problem of the bipolar effect (Fig. 1c). While Bi in SnTe is known to reduce the band gap, in the presence of Pb it opens the band gap of SnTe, and the reason behind this is explained in later sections.[21]

In addition to this, it also introduces a resonance level that appears as a distinct peak near the Fermi level in the density of states (DOS) plot (Fig. 1d).[21,22] These resonance levels are formed due to the hybridization of Bi 'p' states with Sn and Pb 'p' states near the Fermi level just below the conduction band (Fig. 2). In SnTe, we observe that the resonance states introduced by 'p' valence electron impurities are rather broad as seen in this case compared to that of 's' valence electron impurities as seen in the case of Zn resonance levels.[4,22] We also observe that both in $Sn_{11}Pb_5Te_{16}$ and $Sn_{10}Pb_5BiTe_{16}$, the valence bands are formed by Te 'p' orbitals while the conduction band is formed by Sn and Pb 'p' orbitals.[11] In addition to the formation of resonance states, Bi 'p' orbitals are also seen to contribute to the lower conduction bands.

In addition to the low band gap, SnTe suffers drawbacks of high energy offset between the valence sub-bands at the Γ point and $Z + \delta$ in the $Z \rightarrow R$ direction in the supercell. We estimate this band gap to be 0.297 eV in our calculations for SnTe. Doping of Pb leads to further separation of these sub-bands to 0.303 eV, which agrees with a previous report.[11] While several previous reports of Bi doping in SnTe have indicated that there is no decrease in the energy offset of valence sub-bands by the addition of Bi, herein we see that co-doping it with Pb decreases

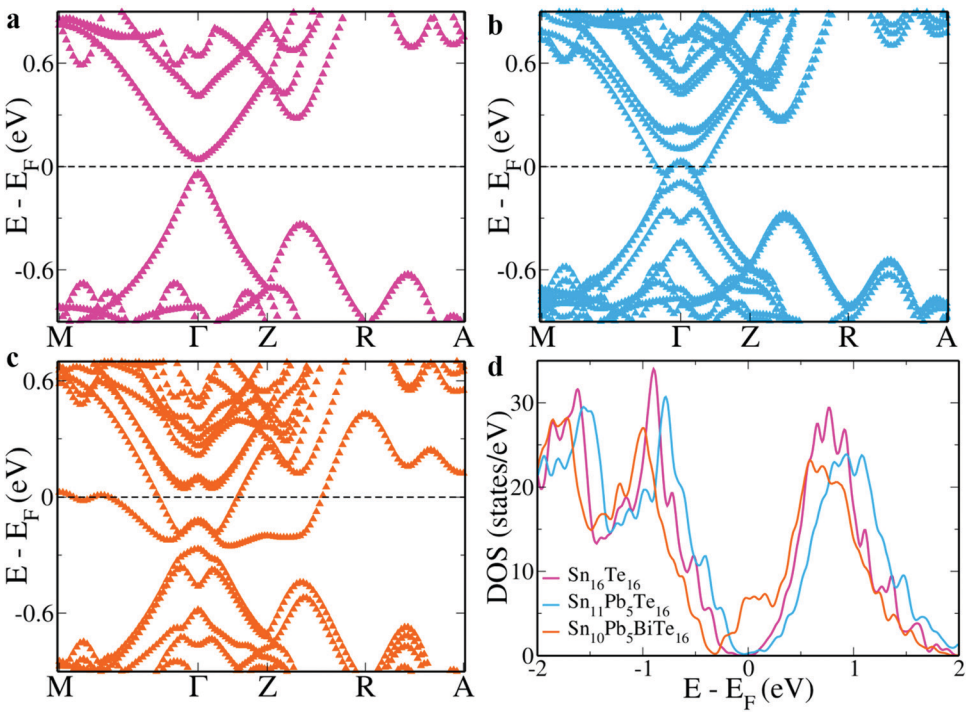

Fig. 1 Electronic structure of (a) $Sn_{16}Te_{16}$; (b) $Sn_{11}Pb_5Te_{16}$; and (c) $Sn_{10}Pb_5BiTe_{16}$; (d) DOS plot of all three configurations. The appearance of a hump near the Fermi level in the DOS plot indicates the formation of a resonance level in $Sn_{10}Pb_5BiTe_{16}$. The energy levels are shifted with respect to the Fermi level, which is set to zero. The L point of the primitive cell folds onto the Γ point and the Σ point folds onto the $Z + \delta$ in the $Z \rightarrow R$ direction in the current supercell.[22]

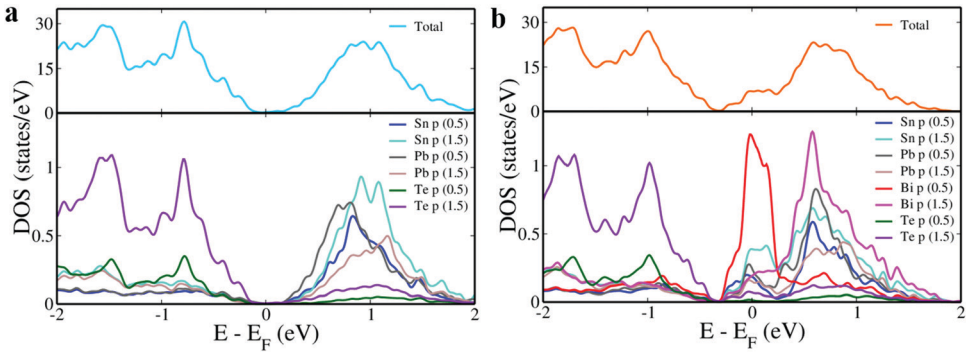

Fig. 2 pDOS of (a) $Sn_{11}Pb_5Te_{16}$; and (b) $Sn_{10}Pb_5BiTe_{16}$. The energy levels are shifted with respect to the Fermi level of the configurations, which is set to zero.

the energy offset value to 0.173 eV.[21,22,28] This unusual behavior of Bi is seen only in the presence of Pb highlighting the importance of choosing the right combination of dopants to engineer the electronic structure.[21,22]

Similar to the valence sub-bands, light and heavy hole conduction sub-bands at the Γ point and $Z + \delta$ in the $Z \rightarrow R$ direction, respectively have a large energy offset in SnTe compared to that in GeTe.[29,30] Note that although the carriers in the conduction bands are electrons the terms light and heavy hole conduction sub-bands are used here to indicate that these are the conduction bands corresponding to the respective light and heavy hole bands in the valence region and it does not mean that the holes are the carriers in the conduction band. We estimate this value to be 0.241 eV in SnTe and 0.233 eV in Pb doped SnTe. While the lowermost valence and conduction bands are eight-fold degenerate, doping of Pb leads to the loss of degeneracy with the bands splitting into 4 doubly degenerate ones in both the valence and conduction band regions. In Pb doped SnTe the lowermost degenerate band caps the valence band making it seem metallic. We observe that with Bi co-doping, this band forms the resonance level and the second set of doubly degenerate bands lying 0.071 eV above the first set in Pb doped SnTe, now form the conduction band edge flanked by the resonance states at the bottom. This leads to an increase in the band gap at the Γ point. The formation of a resonance level drags the heavy hole conduction sub-band lower by 0.087 eV from the Γ point and almost in line with the resonance band protrusions on either side of the Γ point. Such a feature of

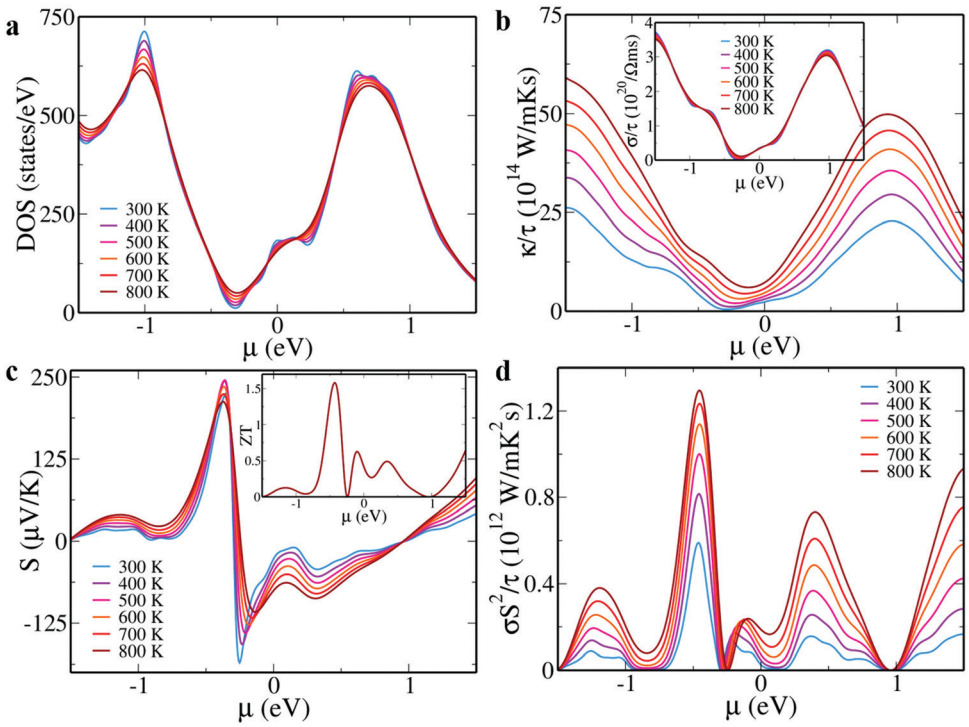

Fig. 3 (a) DOS; (b) thermal conductivity (inset: electrical conductivity); (c) Seebeck co-efficient (inset: ZT@800 K) and (d) power factor of $Sn_{10}Pb_5BiTe_{16}$ as a function of chemical potential (μ) at various temperatures. The conductivity and power factor values are reported by scaling it with τ.

extreme convergence was not reported previously in Bi doped SnTe materials.[31]

Due to the competing traits of electrical conductivity 'σ' and Seebeck coefficient 'S', the power factor 'σS^2' is largely dependent on the electronic structure.[32] The interesting features shown by $Sn_{10}Pb_5BiTe_{16}$ made us curious to study its transport properties using the Boltztrap code under rigid band approximation.[33] We determined DOS, 'σ', 'S', 'σS^2' and 'κ' as a function of chemical potential 'μ' under a constant scattering time approximation in the temperature range of 300 K to 800 K (Fig. 3). The negative and positive potentials indicate hole (p-type) and electron (n-type) doping, respectively.[34]

While the DOS and 'σ' do not show much variation with temperature, we observe an increase in the 'κ' values with an increase in the temperature.[35] The large 'S' values along with high power factors indicate the effect of tuning the electronic structure. Distortion in the density of states due to the resonance levels, an increase in the number of degenerate valleys due to the valence and conduction sub-band convergence leading to an increased effective mass and the increase in the band gap observed in the electronic structure, synergistically lead to improved thermopower. The doping of Pb and Bi in the Sn site leads to large mass fluctuations and atomic point defects leading to scattered phonons. This is known to decrease the lattice thermal conductivity.[36,37] By assuming a lattice thermal conductivity of 0.5 W m^{-1} K^{-1}, we estimate ZT values of $\sim$1.58 at 800 K for the p-type and $\sim$0.63 for the n-type material. Although the material predicts a lower ZT than the combination of Pb with Zn that showed the lowest total thermal conductivity of $\sim$1.5 W m^{-1} K^{-1} and a power factor of $\sim$30.4 μW cm^{-1} K^{-2} at 840 K, by applying strategies like nano structuring, further improvements in the ZT can be achieved. Based on the existing literature reports and the current work, 30 mol% of Pb and 6 mol% of Bi with further tuning of Bi concentration to tune the chemical potential should lead to the realization of high ZT values in the current material. This work opens new opportunities for SnTe based materials as it demonstrates the possibility of achieving better performance in both p and n-type materials by tuning the chemical potential.

4. Conclusions

Herein, we reveal the unusual behavior of a Bi dopant in the presence of Pb in SnTe leading to an enhanced ZT of $\sim$1.58 at 800 K as predicted using Boltzmann transport calculations. We show that, although Pb is known to decrease the thermal conductivity in SnTe, it strengthens the bipolar conduction at high temperatures by closing the band gap of SnTe. However co-doping of Bi leads to an increase in the band gap, eliminating the bipolar effect. Bi in addition to introducing resonance states also causes convergence of the valence and conduction sub-bands in the presence of Pb. Since Bi was not known to cause valence band convergence when doped in SnTe, this behavior is the unique effect of co-doping it with Pb. The electronic structure tuning due to Bi–Pb co-doping leads to the development of a material that can be envisaged to act as both a p and n-type material by tuning the chemical potential.

Conflicts of interest

The authors declare no competing financial interest.

Acknowledgements

The authors gratefully acknowledge the financial support received from CSIR, the Govt. of India in the form of an R&D project grant and DST, Govt. of India for the INSPIRE Faculty award.

References

1 C. Qin, L. Cheng, Y. Xiao, C. Wen, B. Ge, W. Li and Y. Pei, Substitutions and dislocations enabled extraordinary n-type thermoelectric PbTe, *Mater. Today Phys.*, 2021, **17**, 100355.
2 D. K. Bhat and U. S. Shenoy, Enhanced Thermoelectric Performance of Bulk Tin Telluride: Synergistic Effect of Calcium and Indium Co-Doping, *Mater. Today Phys.*, 2018, **4**, 12–18.
3 F. Guo, B. Cui, C. Li, Y. Wang, J. Cao, X. Zhang, Z. Ren, W. Cai and J. Sui, Ultrahigh Thermoelectric Performance in Environmentally Friendly SnTe Achieved through Stress-Induced Lotus-Seedpod-Like Grain Boundaries, *Adv. Funct. Mater.*, 2021, **31**, 2101554.
4 D. K. Bhat and U. S. Shenoy, Zn: A Versatile Resonant Dopant for SnTe Thermoelectrics, *Mater. Today Phys.*, 2019, **11**, 100158.
5 M. Hong, Y. Wang, S. Xu, X. Shi, L. Chen, J. Zou and Z. G. Chen, Nanoscale pores plus precipitates rendering high-performance thermoelectric $SnTe_{1-x}Se_x$ with refined band structures, *Nano Energy*, 2019, **60**, 1–7.
6 S. K. Kihoi and H. S. Lee, Nanostructuring SnTe to Improve Thermoelectric Properties through Zn and Sb Co-doping, *Sustainable Energy Fuels*, 2020, **4**, 5645–5653.
7 G. Wu, Z. Guo, Q. Zhang, X. Wang, L. Chen, X. Tan, P. Sun, G. Q. Liu, B. Yu and J. Jiang, Refined Band Structure Plus Enhanced Phonon Scattering Realizes Thermoelectric Performance Optimization in CuI–Mn Co-doped SnTe, *J. Mater. Chem. A*, 2021, **9**, 13065–13070.
8 J. Tang, B. Gao, S. Lin, J. Li, Z. Chen, F. Xiong, W. Li, Y. Chen and Y. Pei, Manipulation of Band Structure and Interstitial Defects for Improving Thermoelectric SnTe, *Adv. Funct. Mater.*, 2018, **28**, 1803586.
9 X. Li, J. Liu, S. Li, J. Zhang, D. Li, R. Xu, Q. Zhang, X. Zhang, B. Xu, Y. Zhang, F. Xu and G. Tang, Synergistic band convergence and endotaxial nanostructuring: Achieving ultralow lattice thermal conductivity and high figure of merit in ecofriendly SnTe, *Nano Energy*, 2020, **67**, 104261.
10 S. Li, J. Xin, A. Basit, Q. Long, S. Li, Q. Jiang, Y. Luo and J. Yang, *In Situ* Reaction Induced Core–Shell Structure to Ultralow κ_{lat} and High Thermoelectric Performance of SnTe, *Adv. Sci.*, 2020, **7**, 1903493.

11 D. K. Bhat and U. S. Shenoy, SnTe Thermoelectrics: Dual Step Approach for Enhanced Performance, *J. Alloys Compd.*, 2020, **834**, 155181.
12 J. Tang, Z. Yao, Y. Wu, S. Lin, F. Xiong, W. Li, Y. Chen, T. Zhu and Y. Pei, Atomic Disordering Advances Thermoelectric Group IV Telluride Alloys with A Multi-Band Transport, *Mater. Today Phys.*, 2020, **15**, 100247.
13 L. Hu, Y. Zhang, H. Wu, J. Li, Y. Li, M. Mckenna, J. He, F. Liu, S. J. Pennycook and X. Zeng, Entropy Engineering of SnTe: Multi-Principal-Element Alloying Leading to Ultralow Lattice Thermal Conductivity and State-of-the-Art Thermoelectric Performance, *Adv. Energy Mater.*, 2018, **8**, 1802116.
14 R. Moshwan, W. D. Liu, X. L. Shi, Y. P. Wang, J. Zou and Z. G. Chen, Realizing High Thermoelectric Properties of SnTe *via* Synergistic Band Engineering and Structure Engineering, *Nano Energy*, 2019, **65**, 104056.
15 R. Moshwan, W. D. Liu, X. L. Shi, Q. Sun, H. Gao, Y. P. Wang, J. Zou and Z. G. Chen, Outstanding Thermoelectric Properties of Solvothermal-synthesized $Sn_{1-3x}In_xAg_{2x}Te$ Micro-crystals Through Defect Engineering and Band Tuning, *J. Mater. Chem. A*, 2020, **8**, 3978–3987.
16 D. K. Bhat and U. S. Shenoy, High Thermoelectric Performance of Co-Doped Tin Telluride Due to Synergistic Effect of Magnesium and Indium, *J. Phys. Chem. C*, 2017, **121**, 7123–7130.
17 G. Tan, L. D. Zhao, F. Shi, J. W. Doak, S. H. Lo, H. Sun, C. Wolverton, V. P. Dravid, C. Uher and M. G. Kanatzidis, High Thermoelectric Performance of p-type SnTe *via* a Synergistic Band Engineering and Nanostructuring Approach, *J. Am. Chem. Soc.*, 2014, **136**, 7006–7017.
18 S. Roychowdhury, S. U. Shenoy, U. V. Waghmare and K. Biswas, An enhanced seebeck coefficient and high thermoelectric performance in p-type In and Mg co-doped $Sn_{1-x}Pb_xTe$ *via* the co-adjuvant effect of the resonance level and heavy hole valence band, *J. Mater. Chem. C*, 2017, **5**, 5737–5748.
19 S. Roychowdhury and K. Biswas, Effect of In and Cd co-doping on the thermoelectric properties of $Sn_{1-x}Pb_xTe$, *Mater. Res. Express*, 2019, **6**, 104010.
20 Z. Zhou, J. Yang, Q. Jiang, Y. Luo, D. Zhang, Y. Ren, X. He and J. Xin, Multiple effects of Bi doping in enhancing the thermoelectric properties of SnTe, *J. Mater. Chem. A*, 2016, **4**, 13171–13175.
21 U. S. Shenoy and D. K. Bhat, Electronic Structure Engineering of Tin Telluride Through Co-Doping of Bismuth and Indium for High Performance Thermoelectrics: A Synergistic Effect Leading to Record High Room Temperature *ZT* in Tin Telluride, *J. Mater. Chem. C*, 2019, **7**, 4817–4821.
22 U. S. Shenoy and D. K. Bhat, Bi and Zn Co-doped SnTe Thermoelectrics: Interplay of Resonance Levels and Heavy Hole Band Dominance Leading to Enhanced Performance and A Record High Room Temperature *ZT*, *J. Mater. Chem. C*, 2020, **8**, 2036–2042.
23 P. Giannozzi, S. Baroni, N. Bonini, M. Calandra, R. Car, C. Cavazzoni, D. Ceresoli, G. L. Chiarotti, M. Cococcioni and I. Dabo, *et al.*, Quantum ESPRESSO: A Modular and Open-Source Software Project for Quantum Simulations of Materials, *J. Phys.: Condens. Matter*, 2009, **21**, 395502.
24 J. P. Perdew, K. Burke and M. Ernzerhof, Generalized Gradient Approximation Made Simple, *Phys. Rev. Lett.*, 1996, **77**, 3865.
25 S. Y. Xu, C. Liu, N. Alidoust, M. Neupane, D. Qian, I. Belopolski, J. D. Denlinger, Y. J. Wang, H. Lin, L. A. Wray, G. Landolt, B. Slomski, J. H. Dil, A. Marcinkova, E. Morosan, Q. Gibson, R. Sankar, F. C. Chou, R. J. Cava, A. Bansil and M. Z. Hasan, Observation of a topological crystalline insulator phase and topological phase transition in $Pb_{1-x}Sn_xTe$, *Nat. Commun.*, 2012, **3**, 1192.
26 S. Shenoy and D. K. Bhat, Enhanced Bulk Thermoelectric Performance of $Pb_{0.6}Sn_{0.4}Te$: Effect of Magnesium Doping, *J. Phys. Chem. C*, 2017, **121**, 20696–20703.
27 U. S. Shenoy and D. K. Bhat, Electronic Structure Modulation of $Pb_{0.6}Sn_{0.4}Te$ *via* Zinc Doping and Its Effect on the Thermoelectric Properties, *J. Alloys Compd.*, 2021, **872**, 159681.
28 S. K. Kihoi, J. N. Kahiu, H. Kim, U. S. Shenoy, D. K. Bhat, S. Yi and H. S. Lee, Optimized Mn and Bi Co-Doping in SnTe Based Thermoelectric Material: A Case of Band Engineering and Density of States Tuning, *J. Mater. Sci. Technol.*, 2021, **85**, 76–86.
29 D. K. Bhat and U. S. Shenoy, Mg/Ca Doping Ameliorates the Thermoelectrics Properties of GeTe: Influence of Electronic Structure Engineering, *J. Alloys Compd.*, 2020, **834**, 155989.
30 D. K. Bhat and U. S. Shenoy, Resonance Levels in GeTe Thermoelectrics: Zinc as a New Multifaceted Dopant, *New J. Chem.*, 2020, **44**, 17664–17670.
31 S. K. Kihoi, U. S. Shenoy, D. K. Bhat and H. S. Lee, Complimentary Effect of Co-doping Aliovalent Elements Bi and Sb in Self-compensated SnTe-based Thermoelectric Materials, *J. Mater. Chem. C*, 2021, **9**, 9922–9931.
32 S. U. Shenoy and D. K. Bhat, Electronic Structure Engineering of $SrTiO_3$*via* Rhodium doping: A DFT Study, *J. Phys. Chem. Solids*, 2021, **148**, 109708.
33 G. K. H. Madsen and D. J. Singh, BoltzTrap. A code for Calculating Band Structure Dependent Quantities, *Comput. Phys. Commun.*, 2006, **175**, 67–71.
34 U. S. Shenoy and D. K. Bhat, Vanadium Doped $BaTiO_3$ as High Performance Thermoelectric Material: Role of Electronic Structure Engineering, *Mater. Today Chem.*, 2020, **18**, 100384.
35 U. S. Shenoy and D. K. Bhat, Enhanced Thermoelectric Properties of Vanadium Doped $SrTiO_3$: A Resonant Dopant Approach, *J. Alloys Compd.*, 2020, **832**, 154958.
36 S. X. Lin, X. Tan, H. Shao, J. Xu, Q. Wu, G. Q. Liu, W. H. Zhang and J. Jiang, Ultralow Lattice Thermal Conductivity in SnTe by Manipulating the Electron-phonon Coupling, *J. Phys. Chem. C*, 2019, **123**, 15996.
37 X. Wang, H. Yao, Z. Zhang, X. Li, C. Chen, L. Yin, K. Hu, Y. Yan, Z. Li, B. Yu, F. Cao, X. Liu, X. Lin and Q. Zhang, Enhanced Thermoelectric Performance in High Entropy Alloys $Sn_{0.25}Pb_{0.25}Mn_{0.25}Ge_{0.25}Te$, *ACS Appl. Mater. Interfaces*, 2021, **13**, 18638–18647.